

# Integrin Receptor GPIIb/IIIa Bound State Conformation of the Fibrinogen $\gamma$ -Chain C-Terminal Peptide 400–411: NMR and Transfer NOE Studies<sup>†</sup>

Kevin H. Mayo<sup>\*,‡</sup> and Francis Fan<sup>‡,§</sup>

*Department of Biochemistry, Biomedical Engineering Center, University of Minnesota, 420 Delaware Street, S.E., Minneapolis, Minnesota 55455*

Mary Pat Beavers,<sup>||</sup> Annette Eckardt,<sup>||</sup> Patricia Keane,<sup>||</sup> William J. Hoekstra,<sup>||</sup> and Patricia Andrade-Gordon<sup>||</sup>

*The R. W. Johnson Pharmaceutical Research Institute, Spring House, Pennsylvania 19477*

*Received October 18, 1995; Revised Manuscript Received January 18, 1996<sup>®</sup>*

**ABSTRACT:** The C-terminal dodecapeptide from human fibrinogen  $\gamma$ -chain, residues 400–411, HHLG-GAKQAGDV ( $\gamma$ 12), is known to inhibit fibrinogen-mediated platelet cell aggregation via competitive interactions with platelet glycoprotein integrin receptor GPIIb/IIIa. NMR studies of  $\gamma$ 12 in the presence of purified GPIIb/IIIa (230 kDa) demonstrate that two  $\gamma$ 12 binding states ( $\gamma$ 12-I and  $\gamma$ 12-II) are present on the integrin receptor. The N-terminal sequence HHLG is crucial to formation of  $\gamma$ 12 state I since in a shorter  $\gamma$ -chain octapeptide, GAKQAGDV,  $\gamma$ 12-I is not observed. Addition of the hexapeptide GRGDSP to the  $\gamma$ 12-receptor preparation effectively removes the  $\gamma$ 12-I population, suggesting either that  $\gamma$ 12 and GRGDSP share one binding site or that their binding sites are allosterically linked. Distance geometry calculations using transfer NOEs from  $\gamma$ 12-I ( $\gamma$ 12-II shows practically no NOEs) indicate the presence of helix conformation when bound to the receptor. Line broadening and chemical shift changes relative to free  $\gamma$ 12 suggest that  $\gamma$ 12 interacts with GPIIb/IIIa primarily through N-terminal residues H400 to Q407.

Integrins are cell surface glycoprotein (GP)<sup>1</sup> receptors that mediate cell–cell and extracellular matrix–cell adhesion processes. Each heterodimeric integrin is assembled from a pool of  $\alpha$  and  $\beta$  subunits which can be combined in various permutations. One  $\alpha$  subunit, for example, can form heterodimers with at least five different  $\beta$  subunits (Hynes, 1992). At present, platelets are known to contain five integrins, two of the  $\beta_3$  class and three of the  $\beta_1$  class (Ginsberg et al., 1988; Hynes, 1991). Studies with platelets have been instrumental in elucidating various ligand recognition mechanisms of integrins in general. Platelet integrin GP $\alpha_{IIb}\beta_3$  (GPIIb/IIIa) was among the first of the integrins to be identified (Nurden & Caen, 1974) and expressed in completely recombinant form (Poncz et al., 1987; Zimrin et al., 1988; O'Toole et al., 1989).

In the blood clotting cascade [see review by Davie et al. (1991)], activated platelets adhere to each other via a bridge which is formed when plasma fibrinogen [a 330 000 dalton dimer of three polypeptide chains, i.e.,  $\alpha$ ,  $\beta$ , and  $\gamma$  (Doolittle, 1984)] binds to GPIIb/IIIa receptors from different platelet cells (Bennett et al., 1982; Savage & Ruggeri, 1991). Three potential bridging sites have been identified in the fibrinogen amino acid sequence: two RGD-containing sites (Rouslahti & Pierschbacher, 1987) located on the  $\alpha$ -chain and one non-RGD site located within the  $\gamma$ -chain C-terminal residues 400–411, HHLGGAKQAGDV ( $\gamma$ 12) (Kloczewiak et al., 1984). Using electron microscopy, Weisel et al. (1992) observed that the fibrinogen  $\gamma$ -chain C-terminus, but not regions of the  $\alpha$ -chain containing RGD sequences, interacts with GPIIb/IIIa. Farrell et al. (1992, 1994) also provided evidence that the fibrinogen  $\gamma$ -chain sequence alone is essential for optimal platelet aggregation, whereas the  $\alpha$ -chain RGD sequences are “neither necessary nor sufficient for platelet aggregation.”

Integrin GPIIb/IIIa, however, is a promiscuous receptor which will bind to a wide variety of RGD-containing proteins [e.g., fibrinogen (Kloczewiak et al., 1984); fibronectin (Haverstick et al., 1985; Plow et al., 1985); vitronectin (Pytela et al., 1986); and von Willebrand factor (Ruggeri et al., 1983)] as well as to the fibrinogen  $\gamma$ -chain C-terminal sequence. Three ligand binding sites so far have been identified on GPIIb/IIIa: two RGD binding sites on the  $\beta_3$ -chain (IIIa), residues 119–130 (Ruggeri et al., 1986; Takada et al., 1992; Smith & Cheresch, 1988; Bajt et al., 1992a,b) and residues 211–222 (Charo et al., 1991; Bajt et al., 1992a,b; Lanza et al., 1992), and one  $\gamma$ 12 binding site on

<sup>†</sup> This work benefitted from research grants from the W. W. Smith Charitable Trust, Philadelphia, PA, and from the R. W. Johnson Pharmaceutical Research Institute, Springhouse, PA.

\* Address correspondence to this author.

<sup>‡</sup> University of Minnesota.

<sup>§</sup> In partial fulfillment of the Ph.D. requirements at Thomas Jefferson University. Present address: Division of Immunology, Beckmann Research Institute, City of Hope National Medical Center, Duarte, CA 91010.

<sup>||</sup> The R. W. Johnson Pharmaceutical Research Institute.

<sup>®</sup> Abstract published in *Advance ACS Abstracts*, March 15, 1996.

<sup>1</sup> Abbreviations: NMR, nuclear magnetic resonance; 2D-NMR, two-dimensional NMR spectroscopy; HOHAHA, 2D-NMR homonuclear Hartmann–Hahn spectroscopy; NOE, nuclear Overhauser effect; NOESY, 2D-NMR nuclear Overhauser effect spectroscopy; rf, radio frequency; FID, free induction decay; GP, glycoprotein; GPIIb/IIIa, integrin receptor GP $\alpha_{IIb}\beta_3$ ; SDS, sodium dodecyl sulfate;  $\gamma$ 12, dodecapeptide HHLGGAKQAGDV, derived from the fibrinogen  $\gamma$ -chain C-terminus;  $\gamma$ 8, octapeptide GAKQAGDV, derived from the fibrinogen  $\gamma$ -chain C-terminus; RGD, hexapeptide GRGDSP.

the  $\alpha_{IIb}$ -chain (IIb), residues 294–314 (D'Souza et al., 1990, 1991; Taylor et al., 1992). Other potential RGD interactive sites have been identified by hydrophathy complementary approaches and by monoclonal antibody mapping (Calvete et al., 1991a,b; Gartner et al., 1991).

Short, linear RGD-containing peptides as well as the fibrinogen  $\gamma$ -chain C-terminal dodecapeptide  $\gamma$ 12 can compete with parent fibrinogen for GPIIb/IIIa binding and, depending on the peptide concentration, even activate GPIIb/IIIa–fibrinogen binding (Du et al., 1991). Peptide-induced receptor activation exposes occupancy-dependent antibody binding sites, indicating that *in vitro* activation is associated with ligand-induced conformational changes (Du et al., 1991). In several studies, it has been hypothesized that fibrinogen binding to GPIIb/IIIa may proceed by initial recognition of an RGD-like sequence, recognition-induced conformational change, and then additional high-affinity ligand–receptor interaction(s). The presence of multiple contact points combined with effects of allosteric modulation complicates understanding the fibrinogen-mediated platelet–platelet cell adhesion process.

In the present study, the interaction of fibrinogen  $\gamma$ -chain peptide  $\gamma$ 12 with purified platelet integrin receptor GPIIb/IIIa has been followed by using NMR spectroscopy. Data indicate that the  $\gamma$ -chain peptide does interact with GPIIb/IIIa to allow for two peptide–receptor binding states,  $\gamma$ 12-I and  $\gamma$ 12-II. One of these states,  $\gamma$ 12-I, is eliminated by addition of the RGD-containing peptide, GRGDSP. Transfer NOEs are observed only with  $\gamma$ 12-I. These NOEs provide the basis for distance geometry calculations of the receptor-bound conformation of  $\gamma$ 12-I.

## MATERIALS AND METHODS

**Peptide Synthesis.** Peptides representing amino acid sequences from human fibrinogen  $\gamma$ -chain were synthesized on a Milligen Biosearch 9600 automated peptide synthesizer. The procedures used were based on the Merrifield solid phase system utilizing Fmoc-BOP chemistry (Stewart & Young, 1984). After the sequence had been obtained, the peptide support and side chain protection groups were acid (trifluoroacetic acid and scavenger mixture) cleaved. Crude peptides were analyzed for purity on a Hewlett-Packard 1090M analytical HPLC using a reverse-phase C18 VyDac column. Peptides generally were about 90% pure. Further purification was done on a preparative reverse-phase HPLC C-18 column using an elution gradient of 0%–60% acetonitrile with 0.1% trifluoroacetic acid in water. Peptides then were analyzed for amino acid composition on a Beckman 6300 amino acid analyzer by total hydrolysis of samples using 6 N HCl at 110 °C for 18–20 h.

**GPIIb/IIIa Receptor Purification.** Purified GPIIb/IIIa was isolated by a modified method of Pytela et al. (1986). Briefly, outdated human platelets were washed twice with a solution containing 9 parts 0.15 M NaCl and 1 part 3.8% trisodium citrate (pH 6.5). Platelet pellets were resuspended in cold lysis buffer [PBS, pH 7.3, containing 50 mM octyl glucoside (Sigma) and 3 mM phenylmethylsulfonyl fluoride (PMSF)] and incubated at 4 °C for 15 min. The lysate was centrifuged at 30 000g for 20 min, and the supernatant was applied to a KYGRGDS-Sepharose affinity column. The extract was incubated overnight at 4 °C with the affinity

matrix, and then the column was washed with column buffer (PBS, pH 7.3, containing 25 mM octyl glucoside and 1 mM PMSF). Elution of GPIIb/IIIa was accomplished by washing the column with 10 mM EDTA in the column buffer. The purity of the eluate fractions was determined by SDS–polyacrylamide gel electrophoresis (Laemmli, 1970). Protein bands were stained by Coomassie Blue. Fractions containing GPIIb/IIIa were combined, concentrated, and dialyzed in a 10 mM phosphate buffer containing 1 mM CaCl<sub>2</sub>, pH 6.0. Protein determination was carried out using a BCA protein assay kit (Pierce Chemical Co., IL) according to the manufacturer's instructions.

**GPIIb/IIIa–Fibrinogen Binding Assay.** In order to assess the functionality of purified GPIIb/IIIa before and after NMR experiments, an *in vitro* solid phase GPIIb/IIIa binding assay using biotinylated fibrinogen was employed. This rapid and sensitive assay has been fully characterized and documented by Charo et al. (1991). Fibrinogen binding to immobilized GPIIb/IIIa was found to be divalent cation-dependent and was inhibited by peptides and antibodies known to inhibit the binding of adhesive proteins to GPIIb/IIIa on activated platelets. The dissociation constant of fibrinogen to GPIIb/IIIa was similar to that reported by Parise and Phillips (1985) on reconstituted vesicles and higher than that for GPIIb/IIIa on activated platelets. Reported here is a modified procedure as described by Charo et al. (1991). A 96-well Immulon-2 microtiter plate (Dynatech–Immulon) was coated with 50  $\mu$ L of 1 mM RGD-affinity purified GPIIb/IIIa (effective range 0.5–10  $\mu$ g/mL) in 10 mM HEPES, 150 mM NaCl, pH 7.4, per well. The plate is covered and incubated overnight at 4 °C. The GPIIb/IIIa solution is discarded, 150  $\mu$ L of 5% BSA is added, and the resulting mixture is incubated at room temperature for 1–3 h. The plate is washed extensively with modified Tyrodes buffer. Biotinylated fibrinogen (25  $\mu$ L/well) at 2 $\times$  final concentration. The plate is covered and incubated at room temperature for 2–4 h. Twenty minutes prior to incubation completion, one drop of Reagent A (Vecta Stain ABC Horse Radish Peroxidase kit, Vector Laboratories, Inc.) and one drop Reagent B are added with mixing to 5 mL of modified Tyrodes buffer mix, and the resulting solution is left to stand. The ligand solution is discarded, and the plate is washed (5  $\times$  200  $\mu$ L/well) with modified Tyrodes buffer. Vecta Stain HRP-Biotin-Avidin reagent (50  $\mu$ L/well, as prepared above) is added and incubated at room temperature for 15 min. The Vecta Stain solution is discarded, and the wells are washed (5  $\times$  200  $\mu$ L/well) with modified Tyrodes buffer. Developing buffer (10 mL of 50 mM citrate/phosphate buffer at pH 5.3, 6 mg of *o*-phenylenediamine, 6  $\mu$ L of 30% H<sub>2</sub>O<sub>2</sub>; 50  $\mu$ L/well) is added and incubated at room temperature for 3–5 min, and then 2 N H<sub>2</sub>SO<sub>4</sub> (50  $\mu$ L/well) is added. The absorbance is read at 490 nm.

This receptor binding assay was used before and after NMR studies to ensure the integrity of the integrin. GPIIb/IIIa was found to bind parent fibrinogen in either case. Prior to NMR studies, fibrinogen–receptor binding was inhibited by 1  $\times$  10<sup>−6</sup> M GRGDSP or by 4  $\times$  10<sup>−6</sup> M  $\gamma$ 12. Following NMR experiments, the receptor was still quite active, but fibrinogen–receptor binding sometimes decreased by about 50%.

**NMR Measurements.** Freeze-dried samples for NMR measurements were dissolved in H<sub>2</sub>O/D<sub>2</sub>O (9:1). Peptide concentrations ranged from 0.2 to 10 mM. GPIIb/IIIa

receptor concentration was 0.2 mM. Solution conditions were 50 mM sodium phosphate, 2 mM  $\text{CaCl}_2$ , 10 mM SDS, pH 6. pH was adjusted by adding microliter quantities of NaOD or DCl to the protein sample. For most experiments, the temperature was controlled at 298 K. All NMR spectra were acquired on a Bruker AMX-600 NMR spectrometer.

For sequence-specific assignments, NOESY spectra and HOHAHA spectra obtained by spin-locking with a MLEV-17 sequence (Bax & Davis, 1985) were used. Spectra were acquired in the phase-sensitive mode (States et al., 1982). The water resonance was suppressed by direct irradiation (1 s) at the water frequency during the relaxation delay between scans as well as during the mixing time in NOESY experiments. The majority of the 2D-NMR spectra were collected as 512  $t_1$  experiments, each with 1K or 2K complex data points over a spectral width of 5 kHz in both dimensions with the carrier placed on the water resonance. 64 or 96 scans were generally time averaged per  $t_1$  experiment. The data were processed directly on the Bruker AMX-600 X-32 or offline on a Bruker Aspect-1 or SGI Indigo workstation with Bruker UXNMR or FELIX programs, respectively. Data sets were multiplied in both dimensions by a 30–60°-shifted sine-bell or Lorentzian to Gaussian transformation function and generally zero-filled to 1K in the  $t_1$  dimension prior to Fourier transformation.

NOESY spectra (mixing times of 50 to 500 ms) were analyzed to identify TRNOE cross-peaks of strong, medium, and weak intensity by analyzing one-dimensional projections of selected spectral regions and by cross-peak volume integration (Wüthrich, 1986). The sizes of some broadened NOE cross-peaks also were taken into account and re-scaled up in magnitude if they were found to be broader than average.

**Structural Calculations.** All structural calculations were done on a Silicon Graphics (SGI) Indigo Extreme workstation using an R4400 CPU running with 32 MB of RAM. The correct L-amino acid peptide sequence was built using Insight II/Discover (Biosym Technologies, San Diego, CA). To ensure that the starting peptide geometry was correct, initial structures were minimized without NOE-based restraints using the Discover program. A variable-target function distance geometry procedure (DGII in the Biosym suite of programs) was used (Braun & Go, 1985; Ni, 1994). In the absence of stereospecific resonance assignments, pseudoatom corrections were used in these structural calculations. TRNOE-derived distance constraints were incorporated sequentially, starting with one pair at a time from sets of initial random structures. Final iterations incorporated all distance constraints simultaneously. During calculations, the conjugate gradient method was used to minimize the full-matrix error function. Additional NOEs having low intensity or chemical shift degeneracy were then identified from analysis of interim structural models and used iteratively in later calculations. At the final stage, *in vacuo* molecular dynamics (50 ps) and energy minimization were used to relieve structural irregularities, e.g., bad bond lengths and contacts, and to improve structures. Resulting structures were analyzed and compared on an SGI Indigo Extreme workstation using Insight II. Most structures compared favorably with TRNOE-derived distances (less than 0.5 Å deviations) and with energetically favorable  $\phi, \psi$  angles. Structures that did not meet these criteria were discarded.

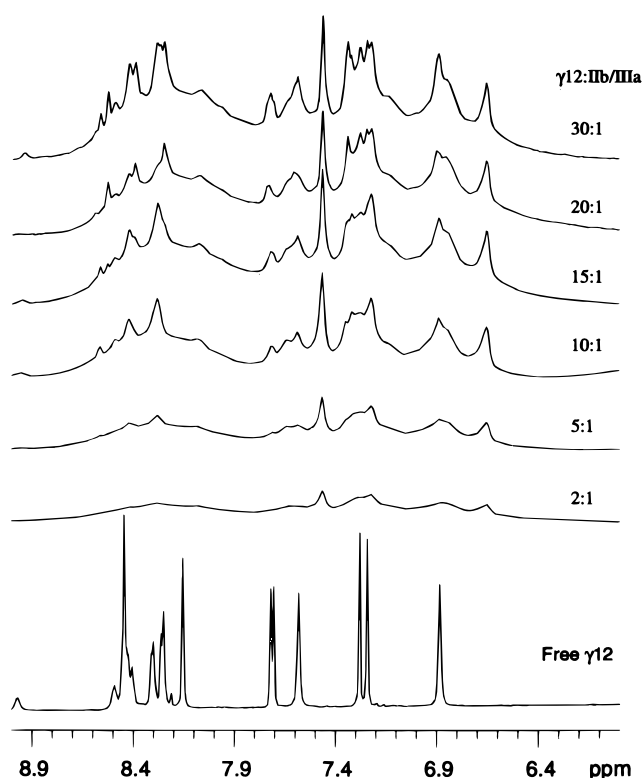


FIGURE 1: NMR spectra for GPIIb/IIIa titration with  $\gamma 12$ . A series of  $^1\text{H}$  NMR spectra are shown for various ratios of  $\gamma 12$ :GPIIb/IIIa (indicated at the right). A spectrum of free  $\gamma 12$  peptide in the absence of GPIIb/IIIa is presented at the bottom. All spectra were acquired under the same solution conditions: 50 mM sodium phosphate, 2 mM  $\text{CaCl}_2$ , 10 mM SDS, pH 6, and 298 K. The GPIIb/IIIa protein concentration was 0.2 mM.

## RESULTS

**Two  $\gamma 12$  Binding States on GPIIb/IIIa.**  $\gamma 12$  titration into a solution containing GPIIb/IIIa produces a series of NMR spectra shown in Figure 1. Proton resonances arising from GPIIb/IIIa (220 kDa) are mostly too broad to be observed although some are apparent, suggesting the presence of a few highly mobile residues. Up to a molar ratio of 5:1 ( $\gamma 12$ :GPIIb/IIIa),  $\gamma 12$  resonances are broadened compared to those from free  $\gamma 12$  (bottom trace). Moreover, chemical shift patterns are significantly different from those found for free  $\gamma 12$ . Increasing the  $\gamma 12$ :GPIIb/IIIa ratio causes resonances to sharpen and to be chemically shifted toward free peptide resonances. This behavior is expected for peptide–receptor interactions that fall in the fast to intermediate ligand exchange regime (London et al., 1992; Campbell & Sykes, 1993; Ni, 1994). Due to chemical shift changes and broadening, resonance assignments cannot be made by direct comparison to 1D-NMR spectra of free  $\gamma 12$ . Furthermore, at ratios of 15:1 and higher, the resonance envelope changes further as additional resonances appear and/or shift. Although the precise amount of GPIIb/IIIa which can bind  $\gamma 12$  peptide is unknown, the ratio of  $\gamma 12$ :GPIIb/IIIa necessary for the observed NMR and TRNOE (see below) effects is consistent with most of the receptor being able to bind peptide (London et al., 1992; Campbell & Sykes, 1993; Ni, 1994).

A HOHAHA spectrum of free  $\gamma 12$  is shown in Figure 2. Sequence-specific resonance assignments (labeled in the figure and listed in Table 1) have been made in the standard way (Wüthrich, 1986) from analysis of HOHAHA and

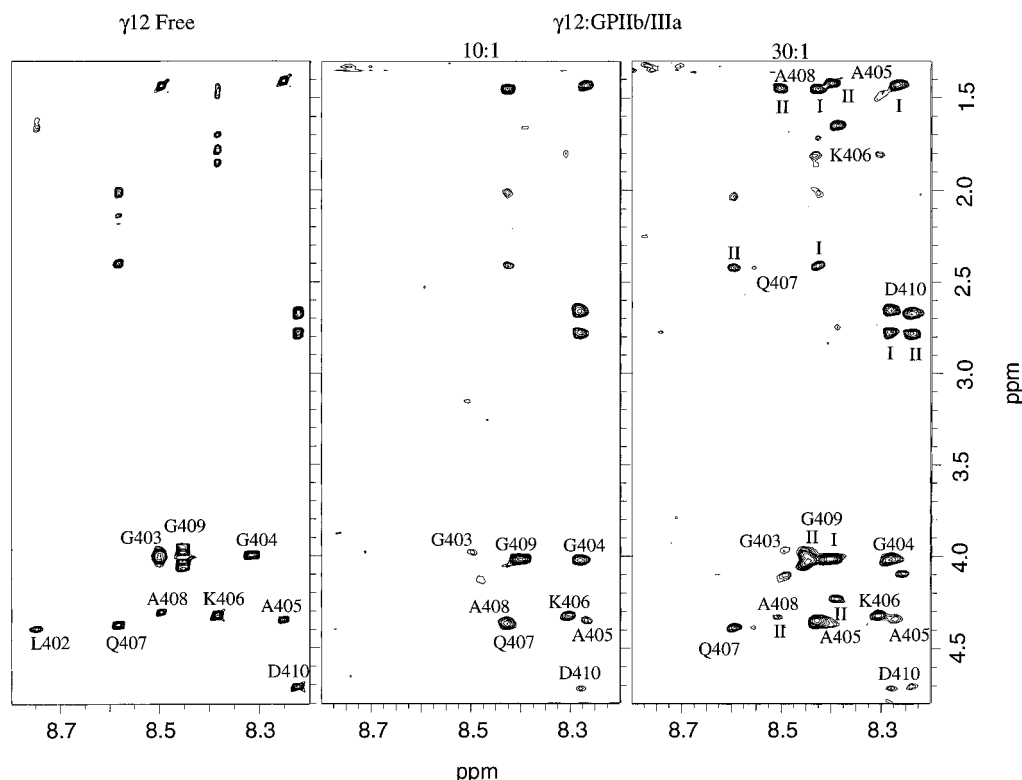


FIGURE 2: HOHAHA spectra of  $\gamma$ 12  $\pm$  GPIIb/IIIa. Three HOHAHA spectra are presented showing the  $\alpha$ H–NH/upfield region for free  $\gamma$ 12 (left panel) and for  $\gamma$ 12:GPIIb/IIIa molar ratios of 10:1 (middle panel) and 30:1 (right panel). Solution conditions are as described in the legend to Figure 1. Free  $\gamma$ 12 peptide concentration was 2 mM, the same concentration as that in the 10:1 ratio spectrum. NMR data were acquired and processed as discussed in Materials and Methods.  $\gamma$ 12 states I and II are labeled as discussed in the text.

Table 1: Chemical Shifts (ppm) for  $\gamma$ 12 in Free and Receptor “Bound” States I and II

residue	NH			$\alpha$ H			$\beta$ H			others		
	bound <sup>a</sup>			bound <sup>a</sup>			bound <sup>a</sup>			bound <sup>a</sup>		
	free	I	II	free	I	II	free	I	II	free	I	II
H400				4.18	4.01		3.19					
H401				4.74	4.73		3.2	3.53				
L402	8.75	8.45		4.40	4.47		1.67	1.82	1.82	$\gamma$ H 1.59	$\gamma$ H 1.65	
										$\delta$ CH <sub>3</sub> 0.91	$\delta$ CH <sub>3</sub> 0.99	
G403	8.50	8.39		4.01	4.15							
					3.96							
G404	8.31	8.28	8.30	4.00	4.01	4.01						
A405	8.25	8.27	8.40	4.36	4.35	4.35	1.41	1.44	1.41			
K406	8.38	8.29	8.44	4.33	4.34	4.34	1.87	1.86	1.86	$\gamma$ CH <sub>2</sub> 1.71	$\gamma$ CH <sub>2</sub> 1.72	$\gamma$ CH <sub>2</sub> 1.72
							1.79	1.72	1.72	$\delta$ CH <sub>2</sub> 1.47	$\delta$ CH <sub>2</sub> 1.48	$\delta$ CH <sub>2</sub> 1.48
										$\epsilon$ CH <sub>2</sub> 3.03	$\epsilon$ CH <sub>2</sub> 3.05	$\epsilon$ CH <sub>2</sub> 3.05
Q407	8.58	8.44	8.60	4.39	4.36	4.38	2.15	2.17	2.17	$\gamma$ CH <sub>2</sub> 2.40	$\gamma$ CH <sub>2</sub> 2.42	$\gamma$ CH <sub>2</sub> 2.42
							2.01	2.02	2.02			
A408	8.50	8.43	8.51	4.31	4.33	4.33	1.44	1.47	1.46			
G409	8.45	8.41	8.46	4.06	4.02	4.04						
				3.98	4.02	4.00						
D410	8.22	8.28	8.23	4.72	4.73	4.73	2.79	2.78	2.79			
							2.69	2.65	2.67			
V411	7.75	7.73	7.73	4.08	4.11	4.11	2.13	2.14	2.14	$\gamma$ CH <sub>3</sub> 0.93	$\gamma$ CH <sub>3</sub> 0.93	$\gamma$ CH <sub>3</sub> 0.93

<sup>a</sup> Chemical shifts are taken at a  $\gamma$ 12:GPIIb/IIIa ratio of 20:1 and have not been extrapolated to 100% bound peptide.

NOESY spectra. H400 and H401 NH resonances are not observed due to their position at the N-terminus and to their resonating near HDO. Histidine C2, C4,  $\alpha$ H, and  $\beta$ H<sub>2</sub> resonances, however, have been resolved in other spectral regions (data not shown). The V411 spin system is observed in HOHAHA spectra but is not shown in Figure 2.

At a  $\gamma$ 12:GPIIb/IIIa ratio of 10:1, a HOHAHA spectrum shows significantly shifted and broadened  $\gamma$ 12 cross-peaks (Figure 2). Even though only one  $\gamma$ 12 binding site on GPIIb/IIIa has so far been reported (D’Souza et al., 1990, 1991;

Taylor et al., 1992), we refer to this  $\gamma$ 12 resonance population as  $\gamma$ 12 binding *state* I (or simply  $\gamma$ 12-I) to acknowledge the possibility that more than one  $\gamma$ 12 binding *site* may be associated with this binding state. Sequence-specific resonance assignments for  $\gamma$ 12-I (Table 1) were made by comparison to chemical shifts for free  $\gamma$ 12 and by using the standard assignment approach with  $\alpha$ N NOESY connectivities. As with free  $\gamma$ 12, H400 and H401  $\alpha$ N HOHAHA and NOESY cross-peaks were absent. In addition, other  $\gamma$ 12-I N-terminal resonances, i.e., L402, G403, and G404, were

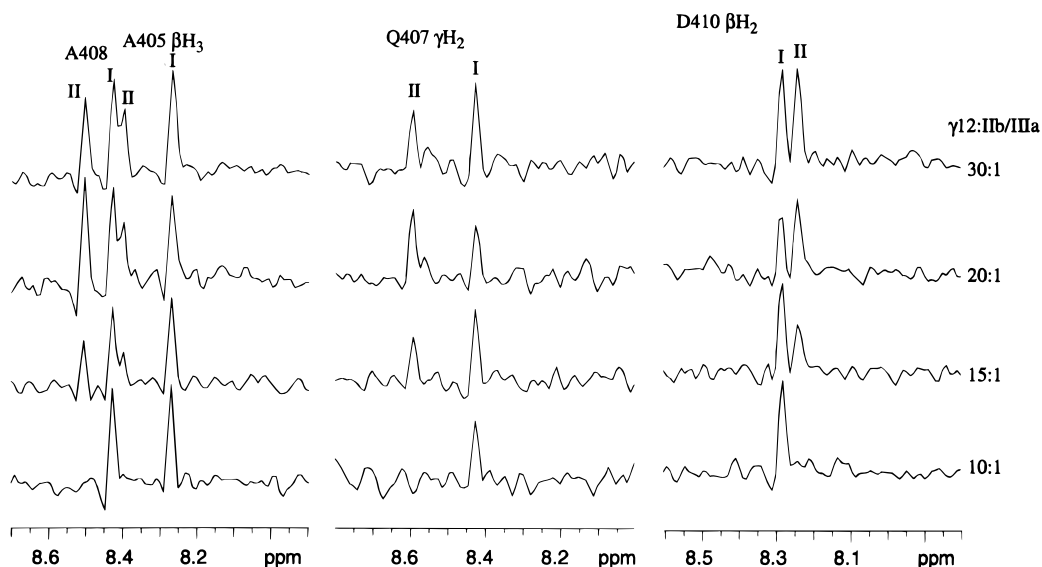


FIGURE 3: 1D HOHAHA slices for  $\gamma 12$  with GPIIb/IIIa. Three series of 1D-NMR spectra are shown for various  $\gamma 12$ :GPIIb/IIIa molar ratios (indicated at the right). Spectra were generated as 1D slices through HOHAHA NH side chain cross-peaks as labeled in the figure.  $\gamma 12$  states I and II are indicated as discussed in the text. Solution conditions are as described in the Figure 1 legend.

not observed in HOHAHA spectra but were present in NOESY spectra. This is probably due to the  $\gamma 12$ :GPIIb/IIIa ratio used and the relatively increased broadening of N-terminal over C-terminal resonances.  $\gamma 12$  line broadening is the result of dynamic exchange (London et al., 1992; Campbell & Sykes, 1993; Ni, 1994) between free  $\gamma 12$  peptide and GPIIb/IIIa receptor-bound peptide.

At a  $\gamma 12$ :GPIIb/IIIa ratio of 30:1, a second  $\gamma 12$  binding state ( $\gamma 12$ -II) is present (Figure 2). Since  $\gamma 12$ -II gave very weak if any  $\alpha N$  NOEs, resonance assignments for the  $\gamma 12$ -II state had to be deduced primarily by comparison to chemical shifts for resonances of free  $\gamma 12$  and bound state  $\gamma 12$ -I. Cross-peaks are labeled as "I" and "II" for interacting states  $\gamma 12$ -I and  $\gamma 12$ -II, respectively. Initially, the observation of highly attenuated (mostly absent) NOEs for  $\gamma 12$ -II was surprising since even free  $\gamma 12$  gave negative (although small) NOEs. This will be addressed later in this section. Chemical shifts for  $\gamma 12$ -II spin systems which could be discerned gave nearly the same chemical shifts as those for free  $\gamma 12$  (see Table 1). Chemical shifts for both  $\gamma 12$ -I and  $\gamma 12$ -II states listed in Table 1 have been taken from data at a 20:1  $\gamma 12$ :GPIIb/IIIa ratio and do not represent extrapolated 100% bound state shifts. The presence of these two  $\gamma 12$  bound states indicates that at least two  $\gamma 12$  binding sites are present on GPIIb/IIIa.

**One  $\gamma 12$  Binding State Induces the Other.** The  $\gamma 12$ -II state appears at higher  $\gamma 12$ :GPIIb/IIIa ratios, after formation of the  $\gamma 12$ -I state. In order to illustrate this point, a more complete  $\gamma 12$ -GPIIb/IIIa titration is shown in Figure 3, which has been generated by taking 1D slices through HOHAHA cross-peaks for A405 and A408 NH- $\beta H_3$ , Q407 NH- $\gamma H_2$ , and D410 NH- $\beta H_2$ . In each case, only  $\gamma 12$ -I resonances are apparent up to a  $\gamma 12$ :GPIIb/IIIa ratio of 10:1, above which  $\gamma 12$ -II resonances are present. In fact,  $\gamma 12$ -II resonances appear to increase in intensity between  $\gamma 12$ :GPIIb/IIIa ratios of 15:1 and 20:1. Continued addition of  $\gamma 12$  above a ratio of 20:1 produces no further spectral changes. These observations suggest that the  $\gamma 12$ -II state may be a direct consequence of the presence of the  $\gamma 12$ -I state. In other words,  $\gamma 12$ -I may induce an allosteric transition in GPIIb/IIIa which promotes formation of the  $\gamma 12$ -

II binding state. This is difficult to say for sure since, with an apparent  $\gamma 12$   $K_d$  value of  $4 \times 10^{-6}$  M, receptor binding sites should be saturated at the  $\gamma 12$ :GPIIb/IIIa 10:1 molar ratio.

The presence of N-terminal residues HHLG is crucial to the presence of the  $\gamma 12$ -I receptor binding state. The absence of these amino acid residues in octapeptide GAKQAGDV ( $\gamma 8$ ) produces only one NMR observable GPIIb/IIIa interacting state (data not shown) showing spectral characteristics consistent with weaker  $\gamma 12$ -receptor interactions. This is corroborated by the  $\gamma 8$   $IC_{50}$  value for inhibition of parent fibrinogen-GPIIb/IIIa binding which is lowered by about 10-fold from  $4 \times 10^{-6}$  M for  $\gamma 12$  to  $40 \times 10^{-6}$  M for  $\gamma 8$ . For this octapeptide that lacks the HHLG sequence, the  $\gamma 12$ -I state is not observed. In this respect, the N-terminal segment that includes the histidines controls formation of the  $\gamma 12$ -I receptor binding state.

**Ligand-Receptor Exchange Time Scales.** Three observations indicate that free  $\gamma 12$  and receptor-bound  $\gamma 12$ -I are in the fast [free  $\rightleftharpoons$  bound] ligand exchange regime: (1)  $\gamma 12$  resonance line widths decrease as the  $\gamma 12$ :GPIIb/IIIa ratio is increased (Figure 1), (2)  $\gamma 12$ -I resonances are chemically shifted relative to those for free  $\gamma 12$  (Figure 2), demonstrating the presence of chemical shift averaging, and shift toward the free state as the  $\gamma 12$ :GPIIb/IIIa ratio is increased, and (3)  $\gamma 12$ -I NOE magnitudes are larger in the presence of GPIIb/IIIa [more negative than for free  $\gamma 12$ ; consistent with the presence of TRNOEs] and decrease as the  $\gamma 12$ :GPIIb/IIIa ratio is increased. This indicates that the receptor off-rate is equal to or greater than about  $100 \text{ s}^{-1}$  (London et al., 1992; Campbell & Sykes, 1993), which is consistent with an apparent equilibrium dissociation constant of  $4 \times 10^{-6}$  M taken from the concentration of  $\gamma 12$  necessary for 50% inhibition of fibrinogen binding to GPIIb/IIIa in the biotinylated fibrinogen binding assay. In this respect, the receptor on-rate would be about  $2.5 \times 10^7 \text{ M}^{-1} \text{ s}^{-1}$ , which is within the expected Stokes-Einstein diffusion-limited range for a 1300 dalton peptide.

Assessing the exchange kinetics (and the origin) of the  $\gamma 12$ -II state is more complicated, and any interpretation must be approached cautiously. If  $\gamma 12$ -II were tightly bound to

GPIIb/IIIa (slow ligand–receptor off-rate), then the bound state NMR signal should disappear for a complex of 220 kDa at a concentration of 0.2 mM, and only free peptide signal would be observed. On the other hand, if there were a rapid equilibrium (fast exchange) between free and bound peptide, then  $\gamma$ 12-II state chemical shifts should represent a weighted average between free and bound forms (London et al., 1992; Campbell & Sykes, 1993; Ni, 1994) as observed for  $\gamma$ 12-I.  $\gamma$ 12-II chemical shifts do vary with respect to those for free  $\gamma$ 12 (Table 1). The best explanation for the tendency of  $\gamma$ 12-II NOEs to be more positive (and mostly absent) relative to those observed for  $\gamma$ 12-I and free  $\gamma$ 12 is an overall slower ligand–receptor off-rate (London et al., 1992; Campbell & Sykes, 1993; Ni, 1994). Regardless of the  $\gamma$ 12-II (and  $\gamma$ 12-I) ligand–receptor exchange time scales, however, free  $\gamma$ 12 peptides (released from GPIIb/IIIa from either state I or state II) should exist in solution in fast exchange with each other, and therefore their respective resonance chemical shifts should represent some weighted average. At higher  $\gamma$ 12:GPIIb/IIIa ratios, results, however, clearly indicate the presence of two  $\gamma$ 12 peptide conformational states (I and II) in slow exchange with each other on the 600 MHz  $^1\text{H}$ -NMR chemical shift time scale.

Although this is unusual, slowly exchanging multiple  $\gamma$ 12 states are not observed in the absence of GPIIb/IIIa or in the presence of SDS alone. Since SDS is known to denature proteins, which could result in artefacts, the conformational integrity of GPIIb/IIIa in the presence of up to 20 mM SDS was checked by both circular dichroism (CD) and fibrinogen binding assay and was found to be unaffected at this SDS:GPIIb/IIIa ratio. GPIIb/IIIa structural/functional integrity was further supported by the ability of GRGDSP to selectively remove the  $\gamma$ 12-I state (described below). SDS had to be used since GPIIb/IIIa, a membrane protein, is relatively insoluble at concentrations required for these experiments without some detergent being present. One possible explanation for this apparent two-state paradox is that ligand binding induces a cis conformation in one or more peptide bonds, resulting in the  $\gamma$ 12-II state. This, however, seems unlikely since  $\gamma$ 12 contains no proline residues and the trans to cis energy barrier for all other amino acid peptide bonds makes such an interconversion extremely unfavorable under conditions of these experiments. An alternative and perhaps more viable explanation is that GPIIb/IIIa (0.2 mM) in the presence of SDS (10 mM) forms a system which mediates slow exchange among receptor-dissociated peptide conformers. SDS alone is known to form micelles under present conditions (Tanford, 1981) and is most likely associating with the receptor. In this scenario, receptor bound peptides from two binding states are released into an SDS/receptor environment which effectively acts to slow down the normally fast conformational exchange among peptides free in solution. In any event, the origin of the  $\gamma$ 12-II state remains unclear.

**RGD Displaces One  $\gamma$ 12 Binding State.** Addition of the hexapeptide GRGDSP at the appropriate  $\gamma$ 12:GPIIb/IIIa ratio effectively eliminates  $\gamma$ 12-I resonances. This is best observed in one-dimensional traces taken from HOHAHA spectra as cross-sections through A405 and A408 NH- $\beta\text{H}_3$  and D410 NH- $\beta\text{H}_2$  cross-peaks as shown in Figure 4. In the absence of GRGDSP,  $\gamma$ 12-I and  $\gamma$ 12-II resonance populations are about equal. At a 1:1 RGD: $\gamma$ 12 ratio, the  $\gamma$ 12-I resonance population is decreased considerably, while

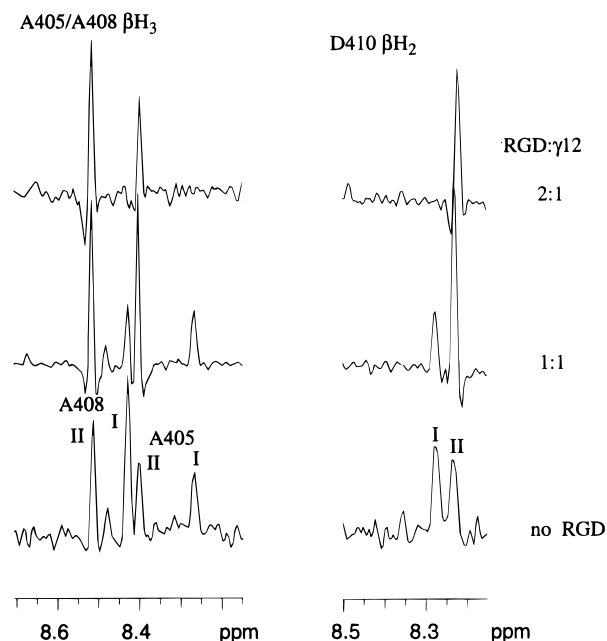


FIGURE 4: NMR spectra for titration with GRGDSP. Two series of 1D-NMR spectra are shown for  $\gamma$ 12 in the presence of GPIIb/IIIa ( $\gamma$ 12:GPIIb/IIIa ratio of 30:1) and at RGD: $\gamma$ 12 molar ratios of 1:1 and 2:1 as indicated at the right in the figure. Spectra were generated as 1D slices through HOHAHA NH side chain cross-peaks as labeled in the figure.  $\gamma$ 12 states I and II are indicated as discussed in the text. Solution conditions are as described in the Figure 1 legend.

at a 2:1 ratio,  $\gamma$ 12-I resonances are not observed. Depletion of  $\gamma$ 12-I resonance intensities at the 2:1 RGD: $\gamma$ 12 ratio is consistent with stronger GRGDSP–receptor binding. In the biotinylated fibrinogen–receptor binding assay, a smaller  $\text{IC}_{50}$  value for GRGDSP relative to that for  $\gamma$ 12 was measured. The most probable interpretations for these results are either that  $\gamma$ 12-I and GRGDSP directly compete for one (or part of one) binding site on GPIIb/IIIa or that their binding sites are allosterically linked. The former explanation is perhaps the more likely since it has been reported (Lam et al., 1987; Ginsberg et al., 1993) that  $\gamma$ 12 and RGD share one (or part of one) binding site on GPIIb/IIIa. On the basis of observations of unaltered  $\gamma$ 12-II NOE magnitudes, binding state  $\gamma$ 12-II appears not to be affected by the presence of GRGDSP.  $\gamma$ 12-II resonances may be shifted slightly due to the  $\gamma$ 12-I and  $\gamma$ 12-II exchange process.

**Transferred NOEs and GPIIb/IIIa Bound State Conformation.** While obviating derivation of the  $\gamma$ 12-II receptor bound state conformation, the near absence of  $\gamma$ 12-II NOEs simplifies NOESY spectral analysis for the  $\gamma$ 12-I state. Aside from  $\gamma$ 12-I  $i,i$  and  $i,i+1$   $\alpha\text{N}$  cross-peaks identified in Figure 5, a number of conformationally constraining NOEs are labeled in Figures 5–7. Free  $\gamma$ 12 NOEs are either smaller or absent relative to those for  $\gamma$ 12-I, and analysis of NOE buildup curves for  $\gamma$ 12-I indicates that maximum NOEs occur at shorter mixing times than for free  $\gamma$ 12. These observations indicate the presence of TRNOEs from  $\gamma$ 12-I due to populations of receptor “bound” peptide in dynamic exchange with free peptide (London et al., 1992; Campbell & Sykes, 1993; Ni, 1994), in agreement with results based on differential line broadening of peptide resonances (Figure 1). Apart from an indication of GPIIb/IIIa binding, the observation of TRNOEs also suggests that the range of conformations accessible to the bound peptide is restricted by the geometry of the binding site on the integrin receptor.

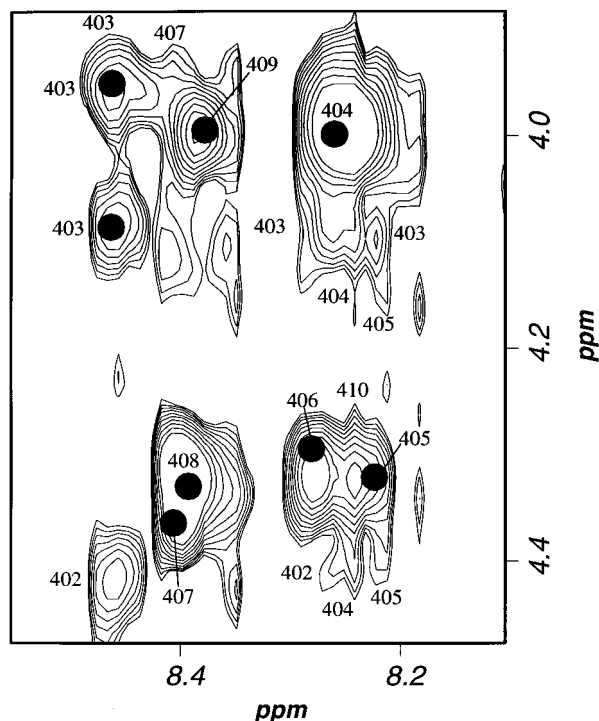


FIGURE 5: NOESY spectrum for  $\gamma 12$ -I receptor bound state. The  $\alpha\text{H}$ -NH region from a NOESY spectrum (200 ms mixing time) is shown. Solution conditions are as described in the legend to Figure 1. NMR data were acquired and processed as discussed in Materials and Methods.  $\gamma 12$ -I state HOHAHA cross-peaks are indicated as filled-in circles and labeled as discussed in the text. Various TRNOEs have been identified.

NOESY spectra (50, 100, 200, and 400 ms) were analyzed to identify TRNOEs and to check for possible spin diffusion. Figure 7 identifies three sequential NH-NH TRNOEs: 403-404, 406-407, and 409-410. By varying solution conditions, we can also observe 405-406 and 407-408 NH-NH TRNOEs (data not shown). At the very least, this series of NH-NH TRNOEs indicates some type of multiple turn or helical conformation in the integrin bound state. Some  $i, i+2$  and  $i, i+3$  TRNOEs which support the presence of helical conformation are identified in Figures 5 and 6. Table 2 lists all  $\gamma 12$ -I TRNOEs. Identification of some potentially informative TRNOEs was precluded by resonance overlap, particularly of  $\alpha\text{H}$  resonances. Using DG-generated structures described below, NOE data were reanalyzed to help identify additional TRNOEs.

TRNOEs have been used to determine the bound structure of  $\gamma 12$ -I. Derivation of TRNOEs can be complicated if the free peptide shows some kind of NOE cross-peaks, especially for sequential and intrasidue interactions (Ni, 1994). In this study, analysis of TRNOEs was simplified considerably since in free  $\gamma 12$ , there were no NOEs greater than  $i, i+1$  and those NOEs which were present were smaller than for the "bound" state. When necessary, corrections were made by subtracting the free  $\gamma 12$  NOE from that of the  $\gamma 12$  bound state NOE. At lower mixing times, free  $\gamma 12$  NOEs represented at most 20% of the uncorrected NOE.

TRNOE cross-peak intensities were classified as strong, medium, weak, or very weak by analyzing one-dimensional F1 and F2 slices from selected NOESY spectral regions and by counting NOESY cross-peak contours (Wüthrich, 1986). The sizes of some broadened NOE cross-peaks also were taken into account and re-scaled up in magnitude if they were

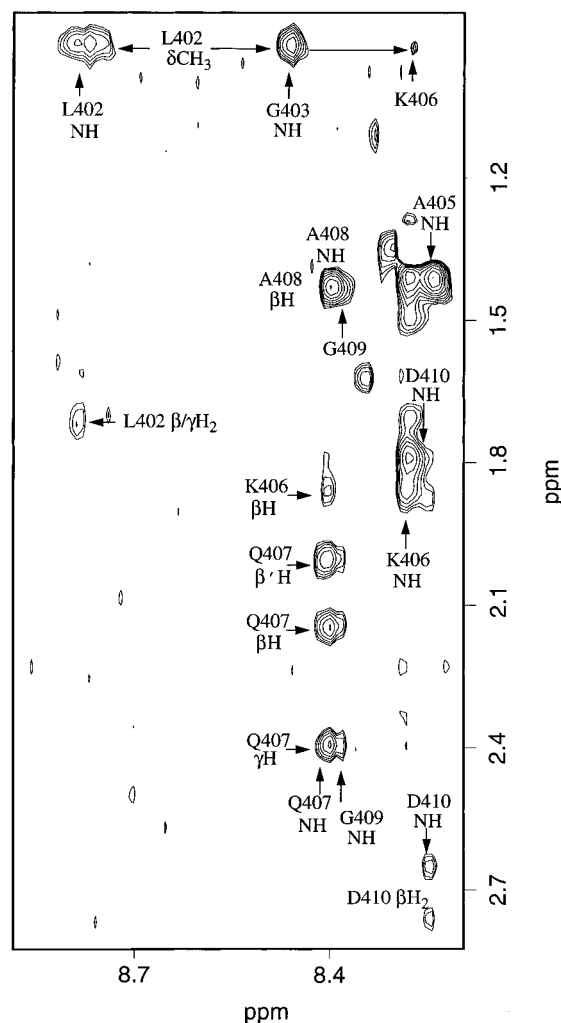


FIGURE 6: NOESY spectrum for  $\gamma 12$ I receptor bound state. The NH- $\beta\text{H}$ /upfield region from a NOESY spectrum (200 ms mixing time) is shown. Solution conditions are as described in the legend to Figure 1. NMR data were acquired and processed as discussed in Materials and Methods. Various TRNOEs have been identified.

found to be broader than average. Increased lower bounds between some sequential  $\alpha\text{H}$ -NH protons also were identified for a few proton pairs which gave smaller NOEs than for free  $\gamma 12$ . Distance cutoffs were then assigned: strong NOEs, 1.8-2.8 Å; medium NOEs, 1.8-3.3 Å; weak NOEs, 1.8-4.0 Å, and very weak NOEs, 1.8-5.0 Å. 0.5 Å was added to the upper limit for each interproton distance involving a side chain. These interproton distances are listed in Table 2. A more quantitative approach was not used primarily because no good distance calibration was available.  $\gamma 12$  contains as aromatics only two histidines whose resonances are not observed, and alanine  $\alpha\text{H}$ - $\beta\text{H}_3$  NOEs could not be determined accurately due to overlap of A405 and A408  $\alpha\text{H}$  resonances. Although the G403  $\alpha\text{H}$ - $\alpha\text{H}$  NOE remained as a potential calibration factor, inaccuracies in TRNOE magnitudes can easily arise with short internuclear distances (Campbell & Sykes, 1993; London et al., 1992; Ni, 1994) as exist between glycine methylene protons [1.8 Å].

On the basis of interproton distances listed in Table 2, a distance geometry (DG) minimization protocol described in the Materials and Methods was used to determine the most probable bound state ensemble of conformations for  $\gamma 12$ -I. Of 50 final structures calculated, the best 35 had favorable

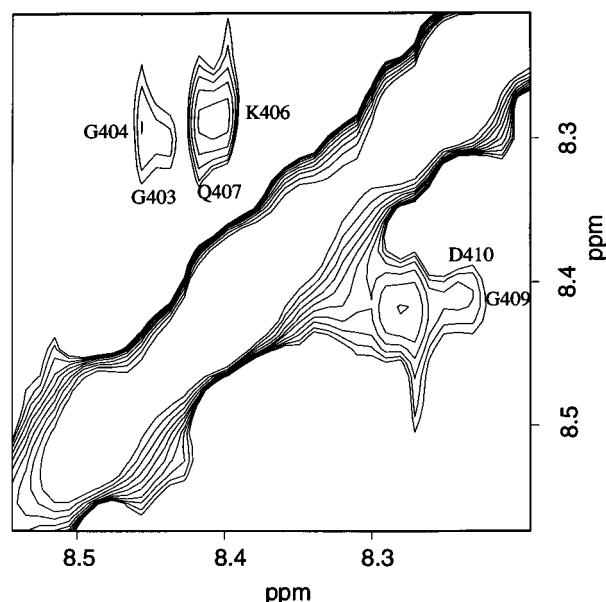


FIGURE 7: NOESY spectrum for  $\gamma$ 12-I receptor bound state. The NH–NH region from a NOESY spectrum (200 ms mixing time) is shown. Solution conditions are as described in the legend to Figure 1. NMR data were acquired and processed as discussed in Materials and Methods. Various TRNOEs have been identified.

Table 2:  $\gamma$ 12–GPIIb/IIIa Transferred NOEs

NOE <sup>a</sup>			NOE <sup>a</sup>		
from	to	size <sup>b</sup>	from	to	size <sup>b</sup>
402 $\alpha$ H	404 NH	w	407 NH	408 NH	m
402 NH	402 $\beta$ H <sub>2</sub>	m		407 $\beta$ H <sup>1</sup>	w
	402 $\delta$ H <sub>2</sub>	m		407 $\gamma$ H <sub>2</sub>	m
403 NH	404 NH	m		403 $\alpha$ H	w
	402 $\delta$ H <sub>3</sub>	w	408 NH	407 $\beta$ H <sub>2</sub>	w
403 $\alpha$ H <sup>2</sup>	405 NH	w		407 $\gamma$ H <sub>2</sub>	w
	406 $\delta$ H <sub>2</sub>	vw		408 $\beta$ H <sub>3</sub>	s
404 $\alpha$ H	406 NH	w		406 $\beta$ H <sub>2</sub>	w
404 NH	402 $\delta$ H <sub>3</sub>	vw	409 NH	408 $\beta$ H <sub>3</sub>	m
	406 $\beta$ H <sub>2</sub>	w		407 $\beta$ H <sub>2</sub>	vw
405 NH	406 NH	m		407 $\gamma$ H <sub>2</sub>	w
	403 $\alpha$ H	w		410 NH	m
	402 $\alpha$ H	w		411 $\gamma$ H <sub>3</sub>	vw
406 NH	406 $\beta$ H <sub>2</sub>	m	410 NH	408 $\alpha$ H	w
	406 $\gamma$ H <sub>2</sub>	m		410 $\beta$ H <sup>1</sup>	m
	406 $\delta$ H <sub>2</sub>	w		407 $\beta$ H <sub>2</sub>	vw
	405 $\beta$ H <sub>3</sub>	m		407 $\gamma$ H <sub>2</sub>	w
	407 NH	m			
	402 $\delta$ H <sub>3</sub>	vw			

<sup>a</sup> NOEs have been tabulated from 100 and 200 ms NOESY spectra accumulated at 25 °C and under conditions as described in the text.  $\alpha$ N  $i, i+1$  NOEs have not been listed since these were not used in structural calculations. <sup>b</sup> Relative NOE magnitudes have been derived from volume integration and/or contour level counting. Lower–upper bound distances used in structural calculations are as follows: strong (s) NOEs, 1.8–2.8 Å; medium (m) NOEs, 1.8–3.3 Å; weak (w) NOEs, 1.8–4.0 Å, and very weak (vw) NOEs, 1.8–5.0 Å. 0.5 Å was added to the upper limit for each interproton distance involving a side chain.

$\phi, \psi$  angles (Richardson, 1981; Iijima et al., 1987) and have been superimposed in Figure 8 by using the backbone heavy atoms of residues G403–G409. Not surprisingly, the N- and C-termini are least defined due to a paucity of NOEs to/from the more terminal residues. Of these 35 structures, 22 superimposed very well with average backbone RMSD values of 0.56 Å (G403–A408). A second subfamily composed of eight other structures also gave good backbone RMSD values (0.68 Å for G403–A408). Another five

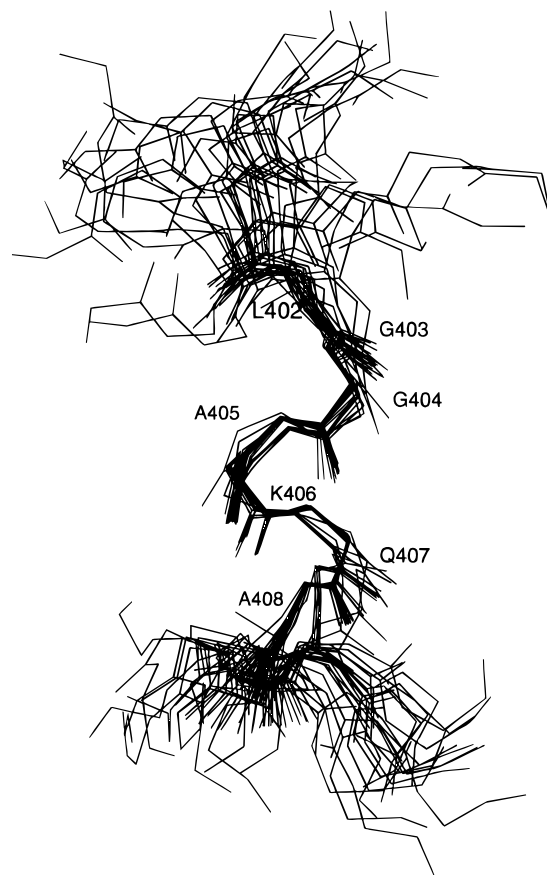


FIGURE 8: Distance geometry calculated structures for  $\gamma$ 12-I. 35 distance geometry calculated structures for the  $\gamma$ 12-I GPIIb/IIIa receptor bound state are overlaid in this figure. DG calculations were performed as discussed in the text. Only backbone heavy atoms have been shown. Residues are labeled close to their C $\alpha$  atoms.

Table 3: Structural Statistics and Atomic RMSD Values

NOE-Derived Distance Restraint Violations (Residues 402–411) <sup>a</sup>			
	no. of restraints	av RMS (Å)	av max (Å) <sup>b</sup>
all <sup>c</sup>	36	0.054	0.28
intraresidue ( $i, i$ )	9	0.048	0.22
sequential ( $i, i+1$ )	10	0.032	0.16
other ( $\geq i, i+2$ )	17	0.071	0.32
Atomic RMSD Values (Å)			
residues	backbone atoms	all heavy atoms	
402–409	0.79	1.93	

<sup>a</sup> No violations greater than 0.4 Å. <sup>b</sup> For residues showing violations; mostly with restraints to side chains. <sup>c</sup> Does not include  $\alpha$ N<sub>( $i, i+1$ )</sub> restraints which were not used in structural calculations. See Table 2.

structures fell close to either subfamily. Table 3 lists some pertinent structural statistics. Among all structures, the conformation from G403 to D410 is best defined as helical.

## DISCUSSION

Understanding ligand–integrin interactions (not to mention integrin-mediated cell adhesion processes) is complicated by the promiscuous nature of these receptors in binding many different ligands, the presence of multiple binding sites, and ligand-induced conformational transitions (Ginsberg et al., 1993). Even working with purified receptor,  $\gamma$ 12 peptide interactions with purified GPIIb/IIIa appear to be no less complicated.



Only one  $\gamma 12$  binding site on the integrin ( $\alpha_{IIb}$  chain) so far had been reported (D'Souza et al., 1990, 1991; Taylor et al., 1992). The present NMR data indicate that  $\gamma 12$  interacts with GPIIb/IIIa on at least two binding sites or states,  $\gamma 12$ -I and  $\gamma 12$ -II. The  $\gamma 12$ -II interaction state appears to be induced by the presence of the  $\gamma 12$ -I state. This may explain why fibrinogen binding to GPIIb/IIIa also can be activated by the presence of peptide ligands (Du et al., 1991). It has been hypothesized that fibrinogen binding to GPIIb/IIIa may proceed by initial recognition of an RGD-like sequence, recognition-induced receptor conformational change(s), and then additional high-affinity ligand-receptor interaction(s) (Du et al., 1993; Ginsberg et al., 1993). Du et al. (1991) found that when soluble purified GPIIb/IIIa is pretreated with  $\gamma 12$  or GRGDSP, the receptor binds fibrinogen with 1:1 stoichiometry and high affinity. This is consistent with the present findings and supports the idea that binding of  $\gamma 12$  to an initial site on GPIIb/IIIa induces an allosteric transition in the receptor which promotes binding at an additional site(s).

The presence of hexapeptide GRGDSP at the appropriate  $\gamma 12$ :GPIIb/IIIa ratio, effectively removes the  $\gamma 12$ -I state without affecting the  $\gamma 12$ -II state. This suggests that the RGD ligand either competes directly with the  $\gamma 12$ -I state or induces a conformational change in the receptor to obviate the  $\gamma 12$ -I interaction state. The former explanation may be more likely. It should be noted that, at higher RGD: $\gamma 12$  ratios, RGD induces formation of up to at least four or five  $\gamma 12$  binding sites on GPIIb/IIIa (Mayo et al., 1996). Lam et al. (1987) have provided evidence that fibrinogen  $\gamma$ -chain C-terminal peptides and RGD-containing peptides do share a common binding site on GPIIb/IIIa. Furthermore, Abrams et al. (1992) found that certain monoclonal antibodies to the idiotype determinant of PAC1 (which binds to GPIIb/IIIa in ways similar to fibrinogen) bind to the  $\gamma$ -chain C-terminus as well as to both  $\alpha$ -chain regions containing RGD sequences. This being the case, one might conclude that in the absence of RGD we are dealing only with two  $\gamma 12$  binding sites on GPIIb/IIIa. In any event, RGD apparently can replace  $\gamma 12$ -I in its role to induce the  $\gamma 12$ -II state. This is consistent with results of Timmons et al. (1989), who reported that platelet receptors interacting with  $\gamma$ - and  $\alpha$ -chains of fibrinogen can be blocked interchangeably by synthetic  $\gamma 12$  and RGD-containing peptides representing sequences on either chain and supports the findings of Weisel et al. (1992) and Farrell et al. (1992) that the  $\gamma$ -chain C-terminal segment alone is essential for optimal fibrinogen-mediated platelet aggregation.

Two RGD ligand binding sequences have been identified on GPIIb/IIIa by chemical/genetic means, and other potential RGD interactive sites have been identified by hydropathic complementary approaches and by monoclonal antibody mapping (Ginsberg et al., 1993). It is unknown, however, if any of these sequences are spatially related, forming fewer actual RGD binding sites. The GPIIb/IIIa  $\gamma 12$ /RGD ligand binding sequences which so far have been identified suggest the importance of oxygenated residues like aspartic acid and serine in the ligand-receptor binding process (Ginsberg et al., 1993). For example, the GPIIIa ( $\beta 3$ ) integrin subunit amino acid sequence D<sup>119</sup>LSYSMKDDLWS<sup>130</sup> is highly conserved among known  $\beta$  subunits (Loftus et al., 1990). Moreover, D<sup>119</sup> is absolutely conserved and is proximal to the residue proposed to be cross-linked to the bound RGD

peptide at K<sup>125</sup> (D'Souza et al., 1988). It has been proposed that the clustering of oxygenated residues could provide coordination sites for various ligands and divalent cations (Kretsinger, 1980; Frelinger et al., 1988). Ginsberg et al. (1993) have hypothesized that oxygenated residues from both the receptor and the ligand are bridged, on interacting, via a divalent cation. The aspartic acid residues in GRGDSP (Ginsberg et al., 1985) and  $\gamma 12$  (D410) (Ruggeri et al., 1986) are given central roles in receptor binding. Alternatively, these are not the only residues found to be crucial to GPIIb/IIIa receptor binding. It has long been held that several other residues in  $\gamma 12$  are crucial for fibrinogen binding to GPIIb/IIIa (Kloczewiak et al., 1989). Substitutions of K406 and V411 are particularly detrimental to bioactivity. Furthermore, Yao and Mayo (1996) recently found that arginines and histidines along with hydrophobic residues on GPIIb/IIIa most probably also mediate fibrinogen binding.

Kloczewiak et al. (1984, 1989) also have noted that even the pentapeptide QAGDV derived from  $\gamma 12$  is only six times less reactive than  $\gamma 12$  in inhibiting fibrinogen-mediated platelet aggregation, while Plow et al. (1984) claim that  $\gamma 12$  without its N-terminal histidines is as reactive as parent  $\gamma 12$  and that shorter peptides derived from  $\gamma 12$  are inactive. While we cannot resolve this controversy, these present NMR studies indicate that the histidines do indeed play a role in  $\gamma 12$  interactions with GPIIb/IIIa. Resonance line broadening and chemical shift changes at any  $\gamma 12$ :GPIIb/IIIa ratio are greatest for  $\gamma 12$  N-terminal residues indicating stronger interactions with GPIIb/IIIa through the N-terminal sequence. Chemical shift differences relative to those of free  $\gamma 12$ , for example, become greater as one moves from the C- to the N-terminus, and G403  $\alpha H_2$  resonances, in fact, become non-degenerate in the bound state. Furthermore, removal of the first four  $\gamma 12$  N-terminal residues (HHLG) produces an eight-residue C-terminal peptide which shows only one GPIIb/IIIa interacting state; the  $\gamma 12$ -I state is apparently eliminated. In this respect, the N-terminal segment that includes the histidines apparently controls formation of the  $\gamma 12$ -I receptor binding state.

TRNOE-derived DG calculated structures for the  $\gamma 12$ -I GPIIb/IIIa bound state can be classified as helical. Earlier NMR studies on a longer  $\gamma$ -chain C-terminal peptide 385–411 (Mayo et al., 1990) provided evidence for helix-like conformation running from 390 through 402, with the C-terminal segment residues 403–411 being less defined due to its high internal mobility. One exception within the flexible C-terminal segment was a turn/loop within the 406–410 sequence. This observation was generally supported by Blumenstein et al. (1993) who found a relatively stable turn centered at residues 408–409 in  $\gamma$ -chain peptide 392–411. This C-terminal segment in  $\gamma$ -chain peptide 385–411 does form additional helix structure that includes the C-terminal segment when the dielectric of the medium is reduced in solutions containing trifluoroethanol (Fan & Mayo, 1995).

Hoekstra et al. (1994, 1995) based the design of a peptide-mimetic GPIIb/IIIa antagonist on the NMR-derived conformation of  $\gamma$ -chain C-terminal residues 385–411 (Mayo et al., 1990). Since the  $\gamma$ -chain 400–411 sequence is required for  $\gamma$ -chain bioactivity and is a unique recognition sequence among ligands for integrins, vis-à-vis other RGD-presenting proteins, these  $\gamma 12$  mimetics may represent a new, selective approach to inhibition of fibrinogen-mediated platelet aggregation. For the rational design phase, the K406, G409

$C_{\alpha}$ – $C_{\alpha}$  distance was maintained between 4.5 and 5 Å with a charge separation of less than 10 Å between the two crucial residues K406 and D410. Although in the present study the receptor-bound conformation for this C-terminal segment 400–411 differs from that for peptide 385–411 (Mayo et al., 1990; Hoekstra et al., 1994, 1995), the K406 to D410 inter-residue distances are essentially the same due to the presence of helical structure. Apparently, electrostatic interactions between K406 and D410 (and/or V411 carboxy terminus) stabilize the observed turn conformation in peptide 385–411 (Mayo et al., 1990). The differences between these structures result from a lack of NOE-derived distance constraints due to the high flexibility of this  $\gamma$ -chain segment noted above. In the receptor bound state, the conformation is “locked-in.”

The  $\gamma$ 12-I receptor bound state conformation defines a surface composed of residues L402–G403, K406–Q407, and D410–V411. The latter four residues were previously identified as being crucial to fibrinogen-mediated platelet–platelet cell adhesion. On the basis of line broadening and chemical shift changes due to the dynamic exchange process between free and bound peptide it is apparent that  $\gamma$ 12 N-terminal residues up to Q407 interact more strongly with GPIIb/IIIa than do the C-terminal residues. These data, therefore, suggest that designing a mimetic that includes elements of this entire surface may make an effective,  $\gamma$ -chain-specific antithrombotic agent.

## CONCLUSIONS

$\gamma$ 12 interacts at two sites on GPIIb/IIIa. Binding at one site apparently induces an allosteric change in GPIIb/IIIa which exposes the second binding site. The presence of the N-terminal histidines is crucial to interactions at the first GPIIb/IIIa binding site. The first occupied site can be competed off with RGD, indicating either that this site is shared with RGD or that RGD induces an allosteric transition to effectively remove this site. The bound state conformation of  $\gamma$ 12 in the first site is helical, placing the important C-terminal lysine, glutamine, aspartic acid, and valine residues on the same surface for interactions with the receptor.

## ACKNOWLEDGMENT

We are very grateful to Eric Eccleston and Denisha Walik of the Department of Human Genetics Microchemical Facility, University of Minnesota, for the synthesis of peptides used in this study. The authors also thank Jeff Press for his support for this project.

## REFERENCES

Abrams, C. S., Ruggeri, Z. M., Taub, R., Hoxie, J. A., Nagaswami, C., Weisel, J. W., & Shattil, S. J. (1992) *J. Biol. Chem.* 267, 2775–2785.  
Adler, M., Lazarus, R. A., Dennis, M. S., & Wagner, G. (1991) *Science* 253, 445–448.  
Andrieux, A., Hudry-Clergeon, G., Ryckewaert, J.-J., Chapel, A., Ginsberg, M. H., Plow, E. F., & Marguerie, G. (1989) *J. Biol. Chem.* 264, 9253–9265.  
Aue, W. P., Bartholdi, E., & Ernst, R. R. (1976) *J. Chem. Phys.* 64, 2229–2246.  
Bajt, M. L., Ginsberg, M. H., Frelinger, A. L., III, Berndt, M. C., & Loftus, J. C. (1992a) *J. Biol. Chem.* 267, 3789–3794.

Bajt, M. L., Loftus, J. C., Gawaz, M. P., & Ginsberg, M. H. (1992b) *J. Biol. Chem.* 267, 22211–22216.  
Bax, A., & Davis, D. G. (1985) *J. Magn. Reson.* 65, 355–360.  
Beer, J. H., Springer, K. T., & Collier, B. S. (1992) *Blood* 79, 117–128.  
Bennett, J. S., Vilaire, G., & Cines, D. B. (1982) *J. Biol. Chem.* 257, 8049–8054.  
Blumenstein, M., Matsueda, G. R., Timmons, S., & Hawiger, J. A. (1992) *Biochemistry* 31, 10692–10698.  
Bradley, E. K., Thomason, J. F., Cohen, F. E., Kosen, P. A., & Kuntz, I. D. (1990) *J. Mol. Biol.* 215, 607–622.  
Braun, W., & Go, N. (1985) *J. Mol. Biol.* 186, 611–623.  
Budzynski, A. Z. (1986) *CRC Crit. Rev. Oncol. Hematol.* 6, 97–146.  
Calvete, J. J., Arias, J., Alvarez, M. V., Lopez, M. M., Henschen, A., & Gonzalez-Rodriguez, J. (1991a) *Biochem. J.* 274, 457–463.  
Calvete, J. J., Arias, J., Alvarez, M. V., Lopez, M. M., Henschen, A., & Gonzalez-Rodriguez, J. (1991b) *Biochem. J.* 273, 767–775.  
Campbell, A. P., & Sykes, B. D. (1993) *Annu. Rev. Biophys. Biomol. Struct.* 22, 99–122.  
Chang, C. T., Wu, C. S. C., & Yang, J. T. (1978) *Anal. Biochem.* 91, 13–31.  
Charo, I. F., Nannizzi, L., Phillips, D. R., Hsu, M. A., & Scarborough, R. M. (1991) *J. Biol. Chem.* 266, 1415–1421.  
Chou, P. Y., & Fasman, G. D. (1978) *Adv. Enzymol. Relat. Areas Mol. Biol.* 48, 45–148.  
Davie, E. W., Fujikawa, K., & Kisiel, W. (1991) *Biochemistry* 30, 10363–10370.  
Doolittle, R. F. (1973) *Adv. Protein Chem.* 27, 1–109.  
Doolittle, R. F. (1984) *Annu. Rev. Biochem.* 53, 195–229.  
D'Souza, S. E., Ginsberg, M. H., Burke, T. A., Lam, S. C.-T., & Plow, E. F. (1988) *Science* 242, 91–93.  
D'Souza, S. E., Ginsberg, M. H., Burke, T. A., & Plow, E. F. (1990) *J. Biol. Chem.* 265, 3440–3446.  
D'Souza, S. E., Ginsberg, M. H., Matsueda, G. R., & Plow, E. F. (1991) *Nature (London)* 350, 66–68.  
Du, X., Plow, E. F., Frelinger, A. L., III, O'Toole, T. E., Loftus, J. C., & Ginsberg, M. H. (1991) *Cell* 65, 409–416.  
Du, X., Gu, M., Weisel, J. W., Nagaswami, C., Bennett, J. S., Bowditch, R., & Ginsberg, M. H. (1993) *J. Biol. Chem.* 268, 23087–23092.  
Dyson, H. J., Rance, M., Houghten, R. A., Lerner, R. A., & Wright, P. E. (1988a) *J. Mol. Biol.* 201, 161–200.  
Dyson, H. J., Rance, M., Houghten, R. A., Wright, P. E., & Lerner, R. A. (1988b) *J. Mol. Biol.* 201, 201–217.  
Fan, F., & Mayo, K. H. (1995) *J. Biol. Chem.* 270, 24693–24701.  
Farrell, D. H., & Thiagarajan, P. (1994) *J. Biol. Chem.* 269, 226–231.  
Farrell, D. H., Thiagarajan, P., Chung, D. W., & Davie, E. W. (1992) *Proc. Natl. Acad. Sci. U.S.A.* 89, 10729–10732.  
Frelinger, A. L., III, Lam, S. C. T., Ploe, E. F., Smith, M. A., Loftus, J. C., & Ginsberg, M. H. (1988) *J. Biol. Chem.* 263, 12397–12402.  
Gartner, T. K., Loudon, R., & Taylor, D. B. (1991) *Biochem. Biophys. Res. Commun.* 180, 1446–1452.  
Ginsberg, M. H., Pierschbacher, M. D., Ruoslahti, E., Marguerie, G. A., & Plow, E. F. (1985) *J. Biol. Chem.* 260, 3931–3936.  
Ginsberg, M. H., Lightsey, A., Kunicki, T. J., Kaufman, A., Marguerie, G. A., & Plow, E. F. (1986) *J. Clin. Invest.* 78, 1103–1111.  
Ginsberg, M. H., Loftus, J. C., & Plow, E. F. (1988) *Thromb. Haemostasis* 59, 1–6.  
Ginsberg, M. H., Frelinger, A. L., III, Lam, S. C.-T., Forsyth, J., McMillan, R., Plow, E. F., & Shattil, S. J. (1990) *Blood* 76, 2017–2023.  
Ginsberg, M. H., Xiaoping, D., O'Toole, T. E., Loftus, J. C., & Plow, E. F. (1993) *Thromb. Haemostasis* 70, 87–93.  
Haverstick, D. M., Cowan, J. F., Yamada, K. M., & Santoro, S. A. (1985) *Blood* 66, 946–952.  
Hermanowski-Vosatka, A., Van Strijp, J. A. G., Swiggard, W. J., & Wright, S. D. (1992) *Cell* 68, 341–352.  
Hoekstra, W. J., Press, J. B., Bonner, M. P., Andrade-Gordon, P., Keane, P. M., Durkin, K. A., Liotta, D. C., & Mayo, K. H. (1994) *Bioorg. Med. Chem. Letters* 4, 1361–1364.

- Hoekstra, W. J., Beavers, M. P., Andrade-Gordon, P., Evangelisto, M. F., Keane, P. M., Press, J. B., Tomko, K. A., Fan, F., Kloczewiak, M., Mayo, K. H., Durkin, K. A., & Liotta, D. C. (1995) *J. Med. Chem.* 38, 1582–1592.
- Hynes, R. O. (1991) *Thromb. Haemostasis* 66, 40–43.
- Hynes, R. O. (1992) *Cell* 69, 11–25.
- Iijima, H., Dunbar, J. B., Jr., & Marshall, G. R. (1987) *Proteins* 2, 330.
- Jeener, J., Meier, B. H., Bachman, P., & Ernst, R. R. (1979) *J. Chem. Phys.* 71, 4546–4553.
- Kessler, H., & Bermel, W. (1986) in *Methods in Stereochemical Analysis 6: Applications of NMR Spectroscopy to Problems in Stereochemistry and Conformational Analysis* (Takenchi, Y., & Marchand, A. P., Eds.) VCH, Deerfield Beach, FL.
- Kloczewiak, M., Timmons, S., Lukas, T. J., & Hawiger, J. (1984) *Biochemistry* 23, 1767–1773.
- Kloczewiak, M., Timmons, S., Bednarek, M. A., Sakon, M., & Hawiger, J. (1989) *Biochemistry* 28, 2915–2919.
- Kretsinger, R. H. (1980) *CRC Crit. Rev. Biochem.* 8, 119–174.
- Laemmli, U. K. (1970) *Nature* 227, 680–685.
- Lam, S. C.-T., Plow, E. F., Smith, M. A., Andrieux, A., Ryckwaert, J.-J., Marguerie, G. A., & Ginsberg, M. H. (1987) *J. Biol. Chem.* 262, 947–950.
- Lanza, F., Stierle, A., Fournier, D., Morales, M., Andre, G., Nurden, A. T., & Cazenave, J. (1992) *J. Clin. Invest.* 89, 1995–2004.
- Loftus, J. C., O'Toole, T. E., Plow, E. F., Glass, A., Frelinger, A. L., III, & Ginsberg, M. H. (1990) *Science* 249, 915–918.
- London, R. E., Perlman, M. E., & Davis, D. G. (1992) *J. Magn. Reson.* 97, 79–98.
- Mayo, K. H., Burke, C., Lindon, J. N., & Kloczewiak, M. (1990) *Biochemistry* 29, 3277–3286.
- Mayo, K. H., Fan, F., Beavers, M. P., Eckardt, A., Keane, P., Hoekstra, W. J., & Andrade-Gordon, P. (1996) *FEBS Lett.* 378, 79–82.
- Ni, F. (1994) *Prog. NMR Spectrosc.* 26, 517–606.
- Nurden, A. T., & Caen, J. P. (1974) *Br. J. Haematol.* 28, 253–260.
- O'Toole, T. E., Loftus, J. C., Plow, E. F., Glass, A., Harper, J. R., & Ginsberg, M. H. (1989) *Blood* 74, 14–18.
- Parise, L. V., & Phillips, D. R. (1985) *J. Biol. Chem.* 260, 10698–10707.
- Parise, L. V., Steiner, B., Nannizzi, L., Criss, A. B., & Phillips, D. R. (1993) *Biochem. J.* 289, 445–451.
- Piantini, U., Sørensen, O. W., & Ernst, R. R. (1982) *J. Am. Chem. Soc.* 104, 6800–6805.
- Plow, E. F., Srouji, A. H., Meyer, D., Marguerie, G., & Ginsberg, M. H. (1984) *J. Biol. Chem.* 259, 5388–5395.
- Plow, E. F., McEver, R. P., Collier, B. S., Woods, V. L., Marguerie, G. A., & Ginsberg, M. H. (1985) *Blood* 66, 724–727.
- Poncz, M., Eisman, R., Heidenreich, R., Silver, S. M., Vilaire, G., Surrey, S., Schwartz, E., & Bennett, J. S. (1987) *J. Biol. Chem.* 262, 8476–8482.
- Pytela, R. P., Pierschbacher, M. D., Ginsberg, M. H., Plow, E. F., & Ruoslahti, E. (1986) *Science* 231, 1559–1562.
- Richardson, J. S. (1981) *Adv. Protein Chem.* 34, 167–186.
- Ruggeri, Z. M., De Marco, L., Gatti, L., Bader, R., & Montgomery, R. R. (1983) *J. Clin. Invest.* 72, 1–12.
- Ruggeri, Z. M., Houghten, R. A., Russell, S. R., & Zimmerman, T. S. (1986) *Proc. Natl. Acad. Sci. U.S.A.* 83, 5708–5712.
- Ruoslahti, E., & Pierschbacher, M. D. (1987) *Science* 238, 491–497.
- Santoro, S. A., & Lawing, W. J., Jr. (1987) *Cell* 48, 867–873.
- Savage, B., & Ruggeri, Z. M. (1991) *J. Biol. Chem.* 266, 11227–11233.
- Shaka, A. J., & Freeman, R. (1983) *J. Magn. Reson.* 51, 161–169.
- Smith, J. W., & Cheresch, D. A. (1988) *J. Biol. Chem.* 263, 18726–18731.
- States, D. J., Haberkorn, R. A., & Ruben, D. J. (1982) *J. Magn. Reson.* 48, 286–293.
- Stewart, J. M., & Young, J. D. (1984) *Solid Phase Peptide Synthesis*, 2nd ed., pp 135, Pierce Chemical Co., Rockford, IL.
- Takada, Y., Ylanne, J., Mandelman, D., Puzon, W., & Ginsberg, M. H. (1992) *J. Cell Biol.* 119, 913–921.
- Tanford, C. (1981) *Physical Chemistry of Macromolecules*, pp 286–296, Wiley, New York.
- Taylor, D. B., & Gartner, T. K. (1992) *J. Biol. Chem.* 267, 11729–11733.
- Timmons, S., Bednarek, M. A., Kloczewiak, M., & Hawiger, J. (1989) *Biochemistry* 28, 2919–2923.
- Weisel, J. W., Nagaswami, C., Vilaire, G., & Bennett, J. S. (1992) *J. Biol. Chem.* 267, 16637–16643.
- Wider, G., Macura, S., Anil-Kumar, Ernst, R. R., & Wuthrich, K. (1984) *J. Magn. Reson.* 56, 207–234.
- Wüthrich, K. (1986) *NMR of Proteins and Nucleic Acids*, Wiley-Interscience, New York.
- Yao, L. J., & Mayo, K. H. (1996) *Biochem. J.* 315, 161–170.
- Zimrin, A. B., Eisman, R., Vilaire, G., Schwartz, E., Bennett, J. S., & Poncz, M. (1988) *J. Clin. Invest.* 81, 1470–1475.

BI952485N